

# Nanonization of Itraconazole by High Pressure Homogenization: Stabilizer Optimization and Effect of Particle Size on Oral Absorption

WEI SUN,<sup>1</sup> SHIRUI MAO,<sup>1</sup> YI SHI,<sup>2</sup> LUK CHIU LI,<sup>2</sup> LIANG FANG<sup>1</sup>

<sup>1</sup>School of Pharmacy, Shenyang Pharmaceutical University, Shenyang, 110016, China

<sup>2</sup>Abbott Laboratories, Abbott Park, Illinois 60064

Received 20 January 2011; revised 21 March 2011; accepted 7 April 2011

Published online 24 April 2011 in Wiley Online Library (wileyonlinelibrary.com). DOI 10.1002/jps.22587

**ABSTRACT:** This study was performed to optimize stabilizer systems used in itraconazole (ITZ) nanosuspensions to achieve the greatest extent of size reduction and investigate the effect of particle size on the *in vitro* dissolution and oral absorption of ITZ. The nanosuspensions were prepared by high pressure homogenization and characterized for particle size, zeta potential, and surface morphology. A central composite method was applied to identify a multiple stabilizer system of Lutrol F127 and sodium lauryl sulfate for optimal particle size reduction. By using the optimized system, an ITZ nanosuspension was prepared that showed the particle size results in good agreement with the values predicted by the model. The nanosuspension was physically stable at 25°C for 1 week. The crystalline form of ITZ was not altered. The ITZ dissolution rate is directly correlated to its particle size, and a smaller particle size yields a faster dissolution rate. Pharmacokinetics study was performed using four ITZ suspensions with various particle sizes in rats ( $n = 3$ ). A significant increase in both maximal plasma concentration of drug and area under the drug concentration–time curve (AUC) was shown when the particle size was reduced from micrometer to nanometer. However, the AUC was not significantly affected by further reduction of the particle size within the nano-size range. © 2011 Wiley-Liss, Inc. and the American Pharmacists Association J Pharm Sci 100:3365–3373, 2011

**Keywords:** nanosuspensions; multiple stabilizer system; central composite design; itraconazole; dissolution; oral absorption

## INTRODUCTION

About half of the new chemical entities generated through combinatorial screening programs are reported to be poorly water-soluble compounds.<sup>1</sup> The dissolution rate is often the rate-limiting step for the oral absorption of these compounds.<sup>2,3</sup> One way to increase the dissolution rate of a poorly water-soluble drug is by reducing its particle size to the nano-size range.<sup>4,5</sup> Nanosuspensions can be defined as colloidal dispersions of submicron pure drug particles that are stabilized by surfactants and/or polymers.<sup>6</sup> A significant increase in the surface area accelerates the dissolution rates of the drugs, leading to improved bioavailability, rapid onset of action, and reduced food effect for BCS Classes II and IV drugs.<sup>7</sup> In the past 10 years,

six nanocrystal-based oral products have been marketed, and quite a number of new products are in different stages of clinical development.<sup>8</sup> The advantages of using the nanosuspension approach include high drug loading capability, simplicity of formulation, absence of cosolvents, and ease of scale up.<sup>7</sup> A highly efficient technology for the preparation of drug nanosuspensions is high pressure homogenization (HPH), which achieves size reduction by the cavitation forces generated when drug dispersion is forced through a very narrow gap under extremely high pressure. The particle size of a nanosuspension manufactured by HPH is controlled by the homogenization pressure, the number of cycles, and the hardness of the drug particles.<sup>9</sup>

Itraconazole (ITZ) is a broad-spectrum triazole antifungal agent, which is widely used for the treatment of blastomycosis, histoplasmosis, onychomycosis, and aspergillosis.<sup>10</sup> ITZ has been classified as a BCS Class II drug,<sup>11</sup> and thus, the bioavailability of

Correspondence to: Shirui Mao (Telephone: +86-24-23986358; Fax: +86-24-23986358; E-mail: shiruimao156@hotmail.com)

Journal of Pharmaceutical Sciences, Vol. 100, 3365–3373 (2011)

© 2011 Wiley-Liss, Inc. and the American Pharmacists Association

unformulated ITZ is extremely low.<sup>12,13</sup> Although ITZ has been employed as a model compound in some research to investigate the physicochemical properties of nanosuspensions, such as drying and surface hydrophobicity characteristics,<sup>14,15</sup> no attempt has been made to systemically evaluate stabilizer systems for optimal size reduction of ITZ in nanosuspensions. Furthermore, the correlation between the *in vitro* dissolution and *in vivo* absorption of ITZ in nanosuspensions as a function of particle size has not been thoroughly investigated. This study was conducted to investigate the impact of stabilizer systems on the size reduction of ITZ nanosuspensions through the use of a central composite statistical design. The aim is to select a stabilizer system that will achieve the most efficient particle size reduction. The effects of particle size on the *in vitro* dissolution and oral absorption of ITZ were also reported.

## MATERIALS AND METHODS

### Materials

Itraconazole (purity 99.5%) was purchased from Tianjin Lisheng Pharmaceutical Company, Ltd. (Tianjin, China). Methocel (hydroxypropyl methylcellulose, HPMC) E15 was a gift from Dow Chemical (Shanghai, China). Lutrol F68 (poloxamer 188), Lutrol F127 (poloxamer 407), and Kollidon 30 (PVP K30) were generously provided by BASF (Shanghai, China). Sodium lauryl sulfate (SLS) and Tween 80 were purchased from Sigma-Aldrich (Shanghai, China). All other chemicals were of analytical grade.

### Preparation of Nanosuspensions

Itraconazole nanosuspensions were prepared by HPH. ITZ coarse powder was first dispersed in an aqueous solution of stabilizer using an Ultra-Turrax T25 (Jahnke & Kunkel, Staufen, Germany) at 8000 rpm for 1 min. The dispersion was then processed through a high pressure homogenizer AH100D (ATS Engineering Inc., Shanghai, China) with two homogenization cycles at 150, 500, and 1000 bar, followed by several cycles at 1350 bar. Nanosuspensions of different particle sizes were prepared by varying the number of homogenization cycles applied.

### Particle Size and Zeta Potential Analysis

The mean particle size ( $z$ -ave) and the polydispersity index (PI) of nanosuspensions were determined by photon correlation spectroscopy (PCS) using a Malvern Zetasizer 4 (Malvern Instruments, Worcestershire, UK) at 25°C and at a scattering angle of 90°. The values were calculated from the cumulants analysis as described in ISO 13321 Part 8 1996 (International Standard on Determination of Particle Size Distributions by PCS). The size distributions displayed

were derived from the correlation functions by analysis with the CONTIN algorithm. The zeta potential measurements were carried out using the Malvern Zetasizer 4 (Malvern Instruments) by electrophoretic laser doppler anemometry at 25°C. The instrument was routinely checked and calibrated using standard reference latex particles (AZ55 Electrophoresis Standard Kit, Malvern Instruments).

### Central Composite Design

A central composite design was performed to investigate the effects of the following two variables on the ITZ particle size reduction: total stabilizers/drug mass ratio ( $X_1$ ) and Lutrol F127/total stabilizers mass ratio ( $X_2$ ). The experimental range of each variable was selected based on the results of preliminary experiments. The data were fitted to a quadratic polynomial model using the Design-Expert software (STAT-EASE Inc., Minneapolis, Minnesota, USA).

### X-Ray Powder Diffraction

X-ray powder diffraction (XRPD) patterns were generated using a D/max 2400 X-ray diffractometer (JEOL, Tokyo, Japan) with Cu K $\alpha$  radiation generated at 40 mA and 35 kV. Samples were analyzed in a  $2\theta$  range of 3°–45° with a step width of 0.04° and a count time of 2 s. The ITZ nanosuspension was lyophilized at a shelf temperature of –50°C with a pressure below 1 mbar for 48 h to obtain a dried sample.

### Differential Scanning Calorimetry

Differential scanning calorimetry (DSC) analysis was performed using a TA-60WS thermal analyzer (Shimadzu, Kyoto, Japan). The ITZ nanosuspension was lyophilized as described above. For the DSC measurements, the samples were weighed into an aluminum pan, which was sealed with a pinhole-pierced cover. Heating curves were recorded at a scan rate of 10°C/min.

### Scanning Electron Microscopy

Morphological examination of ITZ coarse particles was performed using a Quanta 600 scanning electron microscope (FEI, Hillsboro, Oregon, USA), with an accelerating voltage of 20 kV. The ITZ nanosuspension was lyophilized as described above. The lyophilized nanoparticles were examined using a SUPRA 35 field-emission scanning electron microscope (Zeiss, Jena, Germany) at an accelerating voltage of 10 kV. Prior to imaging, the mounted samples were coated with gold under vacuum.

### Short-Term Physical Stability

The physical stability of the nanosuspension at 25°C was evaluated over 1 week period of time. The nanosuspension was kept in a closed glass vial. At the predetermined time intervals, aliquots were taken

and subjected to particle size analysis as described above.

### ***In Vitro* Dissolution**

Dissolution experiments were performed using a USP II apparatus at 37°C and a paddle speed of 50 rpm. The ITZ suspensions (containing 50 mg of ITZ) of various particle sizes were added to dissolution vessels containing 900 mL of 0.1 M HCl. Samples (5 mL) were collected at  $t = 5, 10, 15, 30, 45, 60,$  and 90 min and immediately filtered through a 0.22  $\mu\text{m}$  syringe filter. The concentration of ITZ in each dissolution sample was determined by ultraviolet at 258 nm as previously described.<sup>11</sup> Tests were carried out in triplicate and the results were recorded as an average.

### **Pharmacokinetic Study in Rats**

All animal studies were approved by the Ethics Committee of Shenyang Pharmaceutical University and were conducted in accordance with the National Institute of Health (NIH) Guide for the Care and Use of Laboratory Animals. Four ITZ suspensions with various particle sizes (300 nm, 750 nm, 5.5  $\mu\text{m}$ , and coarse) were administered to male Wistar rats (body weight  $270 \pm 20$  g). All formulations were dosed to rats at a single dose of 30 mg/kg by oral gavage. Serial blood samples were collected over a period of 24 h after dosing at  $t = 0, 1, 2, 3, 4, 5, 6, 8, 12,$  and 24 h and placed into preheparinized microcentrifuge tubes. Plasma samples were harvested by centrifugation at  $3000 \times g$  for 15 min and analyzed according to a previously published high-performance liquid chromatography (HPLC) method.<sup>16,17</sup> The plasma samples were extracted using a heptane–isoamylalcohol (95:5, v/v) mixture by vortex and followed by centrifugation at  $7100g$  for 10 min. The organic layer was then transferred to a new tube and evaporated under a stream of nitrogen. The residue was reconstituted in a HPLC mobile phase. The HPLC assay was carried out using an Agilent 1100 HPLC system (Agilent Technologies, Santa Clara, California, USA). HPLC parameters used to determine ITZ concentration in the plasma samples are listed below.

1. Column: Diamonsil C<sub>18</sub> column ( $150 \times 4.6$  mm<sup>2</sup>, 5  $\mu\text{m}$ ; Dikma Technologies, Beijing, China)
2. Column temperature: 30°C
3. Flow rate: 1 mL/min
4. Wavelength: 263 nm
5. Injection volume: 70  $\mu\text{L}$
6. Mobile phase: 65% acetonitrile, 35% water

The area under the drug concentration–time curve (AUC) was calculated using the trapezoidal rule. The maximal plasma concentration of drug ( $C_{\text{max}}$ ) and the time to reach maximum plasma concentration ( $T_{\text{max}}$ ) were directly obtained from the plasma data.

### **Statistical Analysis**

All the experimental results were depicted as the mean value  $\pm$  standard deviation from at least three measurements. Significance of difference was evaluated using one-way analysis of variance at a probability level of 0.05.

## **RESULTS AND DISCUSSION**

### **Effect of Single Stabilizer**

Both surfactants and polymers have been widely used as stabilizers for nanosuspensions,<sup>18</sup> including non-ionic surfactants such as Poloxamers (Lutrol F68 and F127) and Tween 80, ionic surfactants such as SLS, and polymers such as cellulose (HPMC) and PVP.

The particle size distribution of ITZ nanosuspensions prepared with different stabilizers is shown in Figure 1. The results indicate that polymeric stabilizers were less effective ( $z\text{-ave} > 1500$  nm,  $PI > 0.85$ ) than surfactants ( $z\text{-ave} < 550$  nm,  $PI < 0.35$ ) in terms of particle size reduction. When the results for different nonionic surfactants were compared, F127 was shown to produce the most efficient particle size reduction ( $p < 0.05$ ). It is also interesting to note that there is no significant difference in the final particle size of the nanosuspensions stabilized by F127 or SLS ( $p > 0.05$ ). A stabilizer is usually incorporated in a nanosuspension formulation to prevent or slow down the crystal growth of nanoparticles via Ostwald ripening. However, the impact of stabilizers on the extent of particle size reduction as seen in the present study is unlikely associated with such a stabilization effect because of the extremely short duration of the homogenization process. It seems reasonable to postulate that the degree of dispersion of the drug particles during homogenization can influence the efficiency of particle fragmentation. If particles are staying apart while passing through the narrow gap of the homogenizer, a more efficient particle fragmentation can be achieved. In comparison with polymers, surfactants can provide more effective wetting of the drug particles. This would result in a better dispersion of the drug particles and a greater extent of particle size reduction. The higher molecular weight of F127 (vs. F68 and Tween 80) and its relatively longer polymer chains can lead to a higher degree of steric stabilization for the drug particles, which can enhance particle dispersion and result in a greater extent of size reduction. Although steric stabilization is not associated with SLS, the relatively high zeta potential ( $-30.7$  mV) can keep the drug particles well dispersed via electrostatic repulsion/stabilization. This may explain the more effective size reduction seen in nanosuspensions stabilized with SLS as compared with those stabilized by other nonionic surfactants

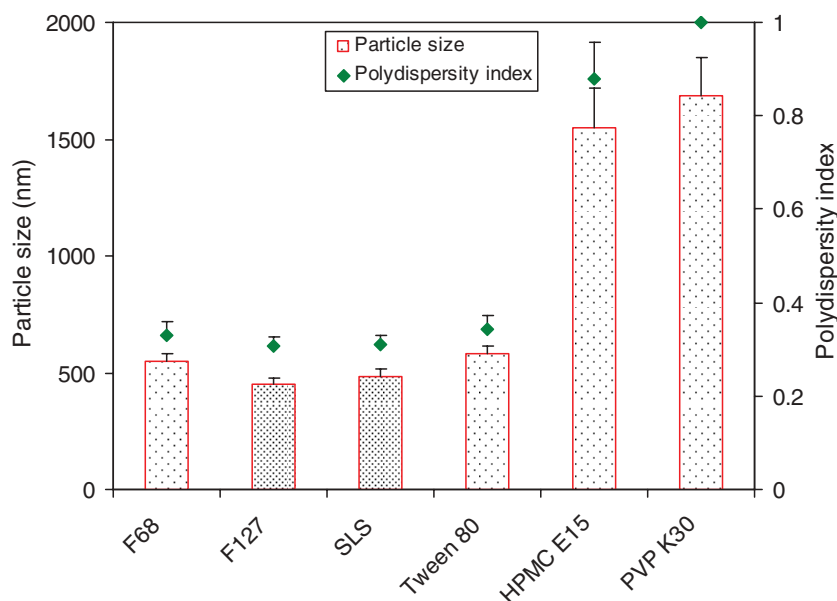


**Figure 1.** The influence of single stabilizer systems (50%, w/w to drug) on the particle size and polydispersity index of itraconazole nanosuspensions (1%, w/w) prepared by HPH.

with a relatively low zeta potential ranging from  $-10$  to  $-20$  mV.

### Effect of Multiple Stabilizer System

On the basis of the results obtained with the single stabilizer systems discussed above, stabilizer system consisting of multiple stabilizers was further investigated. The use of multiple stabilizers was expected to gain the combined advantages of both steric and electrostatic stabilization in achieving a more efficient particle size reduction of ITZ during homogenization. Although the use of multiple stabilizer systems has been reported in some studies on nanosuspensions,<sup>19,20</sup> few of them focused on systemic optimization of the composition of the stabilizer systems. Preliminary experimental results revealed that two factors, total stabilizers/drug mass ratio ( $X_1$ , %) and Lutrol F127/total stabilizers mass ratio ( $X_2$ , %), can significantly affect the mean particle size of ITZ nanosuspensions ( $Y$ , nm). Thus, a central composite statistical design was applied to optimize the multiple stabilizer systems. The response surface and contour plots are presented in Figure 2.

As shown in the plots, with the increase in total stabilizers percentage, nanosuspensions with smaller particle size were obtained; however, after reaching a minimum value, the particle size of the nanosuspensions started to increase. It was also noted that the particle size of the nanosuspensions decreased with an increase in the F127 ratio in the multiple stabilizer system. But, when the F127 ratio was higher than 55%, nanosuspensions with larger particle size were produced. Although a plausible explanation for this complex interaction effect seems to be lacking, it

is likely that a fine balance between the two stabilizers must be achieved to obtain the maximal effect of both steric and electrostatic stabilization for the size reduction of the nanosuspension during homogenization.

In order to achieve the minimum particle size ( $Y$ ), the optimized formulation with  $X_1$  (35%) and  $X_2$  (55%) was selected in the center of the contour plot. The nanosuspension prepared with the optimized formulation yielded a mean particle size of  $315.7 \pm 19.2$  nm with a PI of  $0.272 \pm 0.043$  ( $n = 5$ ), which is in good agreement with the value predicted by the model ( $\sim 320$  nm). This result suggests that the central composite statistical design is a useful tool for predicting the impact of stabilizer composition on the particle size reduction of ITZ nanosuspensions prepared by homogenization. The nanosuspension with the optimized formulation was prepared and used for subsequent characterization and evaluations.

### Evaluation of Crystalline State

The crystalline state of ITZ before and after HPH was examined by XRPD and the results are presented in Figure 3. The XRPD pattern of ITZ nanoparticles was almost identical to that of the coarse ITZ powder, indicating that the high-energy HPH process did not alter the crystalline form of ITZ. DSC analysis was also performed in this study and representative DSC thermograms are presented in Figure 4. The coarse ITZ powder exhibited a sharp melting peak, indicating the crystalline nature of the drug. For the nanoparticle sample, the endothermic peaks at  $56.2^\circ\text{C}$  and  $195^\circ\text{C}$  corresponded to peaks of F127 and SLS, respectively, and the broad endothermic peak at

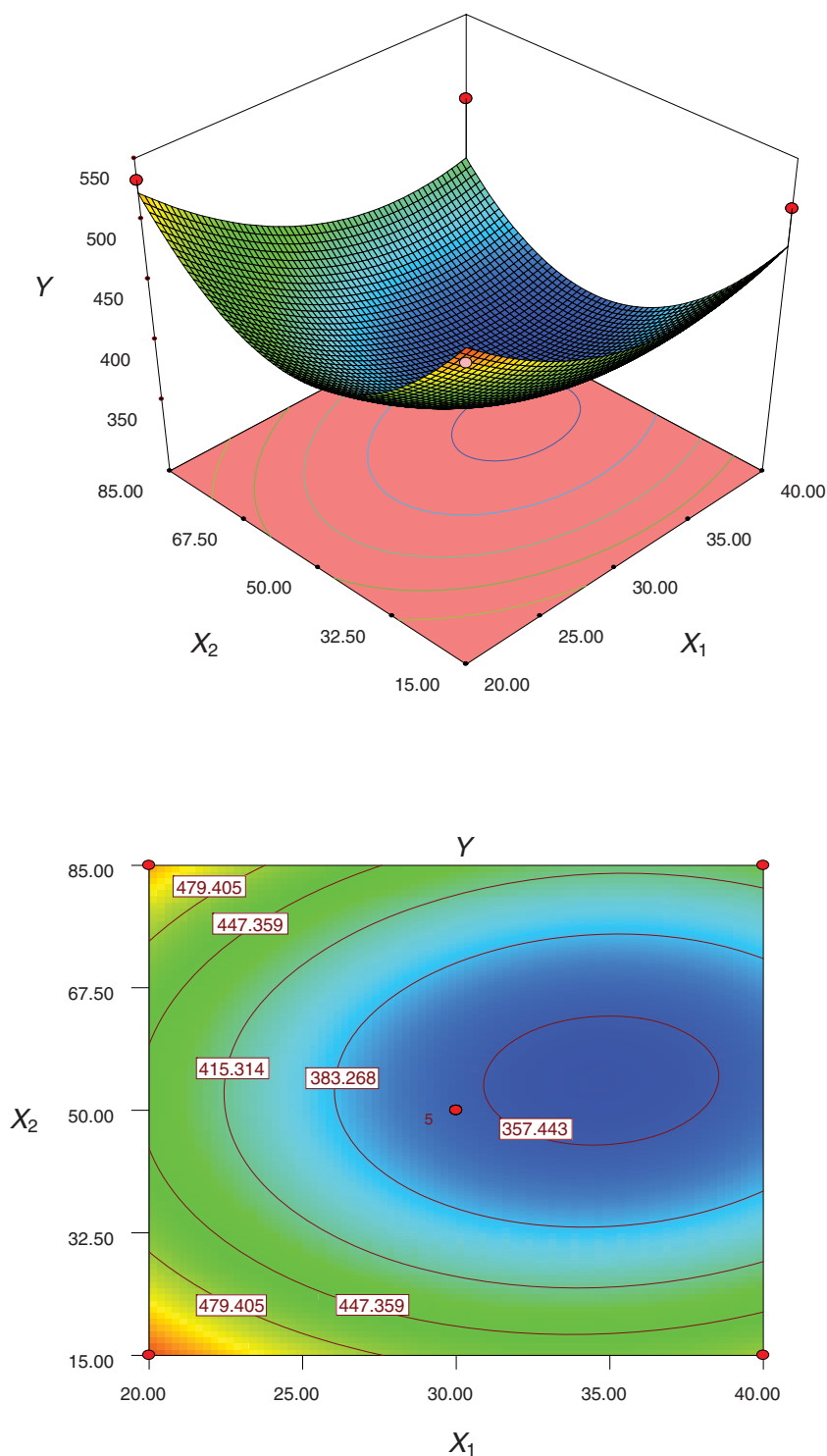


**Figure 2.** Response surface plot (top) and contour plot (bottom) for mean particle size of 1% (w/w) ITZ nanosuspensions ( $Y$ , nm) as functions of two factors: total stabilizers/drug mass ratio ( $X_1$ , %) and Lutrol F127/total stabilizers mass ratio ( $X_2$ , %).

approximately 100°C resulted from the evaporation of moisture from the sample. The ITZ nanoparticles exhibited a sharp endothermic melting peak, indicative of the crystalline structure of the ITZ nanoparticles. Although the crystalline state of ITZ was main-

tained during the HPH process, the onset temperature for the melting of ITZ nanoparticles shifted to a lower value (158.3°C) as compared with the coarse ITZ particles (164.2°C). This phenomenon is probably caused by the depression of the melting point of

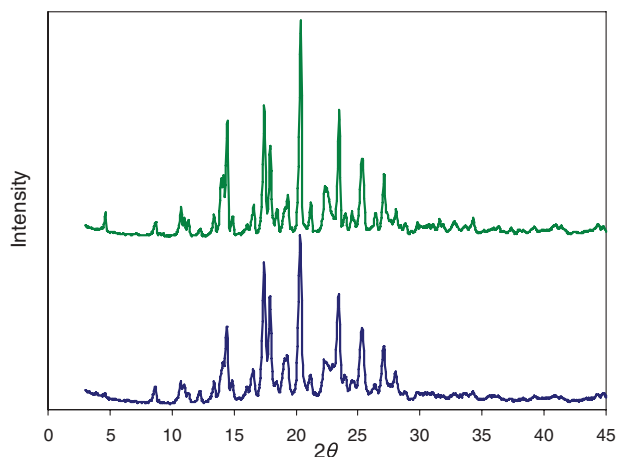


**Figure 3.** X-ray diffraction patterns of coarse itraconazole powders (top) and lyophilized itraconazole nanocrystals prepared by HPH (bottom).

materials in form of small crystals as predicted by the Gibbs–Thomson equation.<sup>21</sup> A similar observation was also reported by other researchers.<sup>22</sup>

The SEM photomicrographs in Figure 5 show the distinctive differences between the coarse powder and the nanoparticles. Plate- and rod-shaped crystals were observed in the coarse ITZ powder, and the particle size was approximately 15  $\mu\text{m}$  with broad size distribution. The HPH converted the coarse particles into nanocrystals with a relatively narrow size distribution. It was also observed that the average size of the ITZ nanocrystals, as seen in the photomicrograph, was approximately 300 nm, which was consistent with the results of PCS analysis.

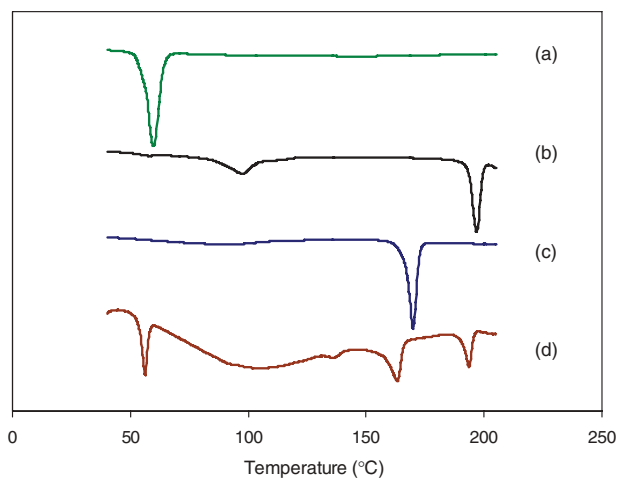


**Figure 4.** Representative DSC thermograms: (a) Lutrol F127, (b) SLS, (c) coarse itraconazole, and (d) lyophilized itraconazole nanosuspension.

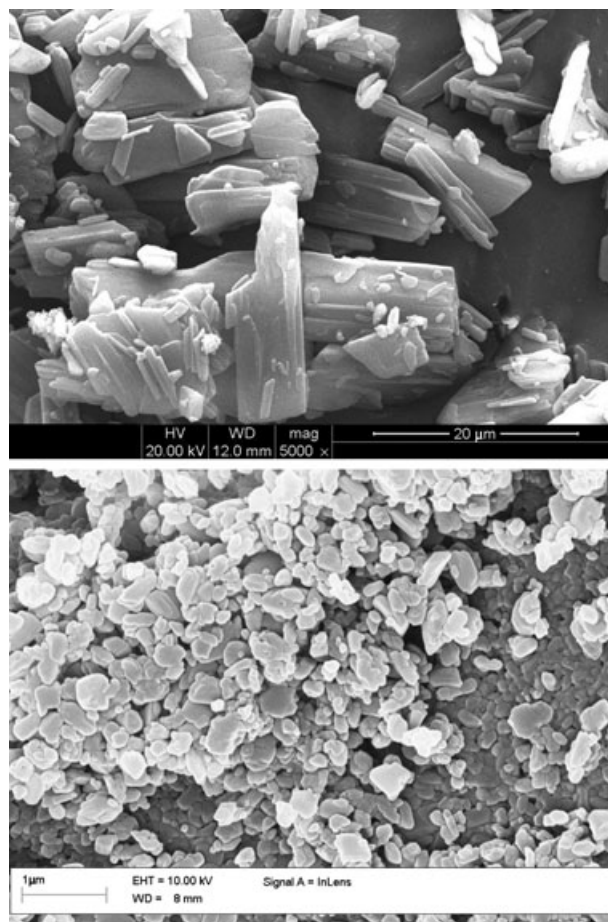


**Figure 5.** Scanning electron microscopy micrographs of coarse itraconazole powders (top) and lyophilized itraconazole nanocrystals prepared by HPH (bottom).

### Short-Term Stability Studies

The short-term physical stability of the ITZ nanosuspension at 25°C was investigated to evaluate whether the nanosuspension was sufficiently stable for further processing such as drying. It was found that there was no significant change in the mean particle size and the PI value when the 300-nm ITZ nanosuspension was stored at 25°C over 1 week. At time zero, the mean particle size was  $318.5 \pm 16.4$  nm with a PI of  $0.283 \pm 0.062$ , and at the 1 week time point, the mean particle size was  $327.2 \pm 17.1$  nm with a PI of  $0.297 \pm 0.073$  ( $p > 0.05$ ). The 750-nm nanosuspension with the same binary stabilizer system as that of 300-nm nanosuspension was also stable for at least 1 week, with no significant change in the mean particle size ( $758.2 \pm 30.7$  vs.  $769.5 \pm 35.1$  nm,  $p > 0.05$ ). As discussed above, the steric and electrostatic repulsive forces between the nanoparticles provided by the binary stabilizer system were able to prevent aggregation of the nanoparticles. This could also prohibit the crystal growth caused by Ostwald ripening, and thus, no change in the particle size of

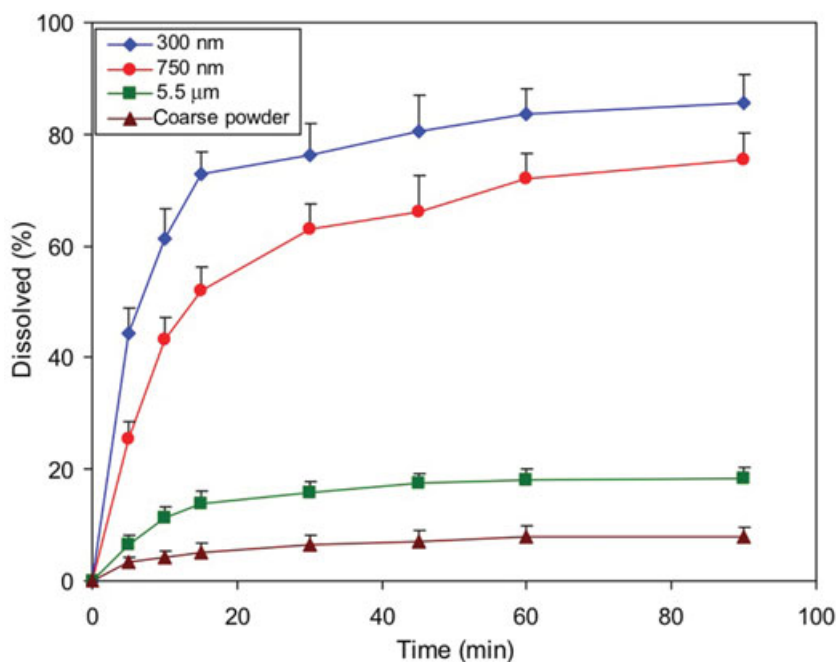


**Figure 6.** *In vitro* dissolution profiles of itraconazole from the suspensions of various particle sizes in 0.1 M HCl at 37°C ( $n = 3$ ).

the nanosuspension was observed. Similarly, it was reported that the good physical stability of ascorbyl palmitate nanosuspensions was attributed to the inhibition of Ostwald ripening by the steric stabilization effect of stabilizers.<sup>23</sup>

#### Effect of Particle Size on *In Vitro* Dissolution

The *in vitro* dissolution profiles of ITZ suspensions with different particle sizes are shown in Figure 6. The dissolution of ITZ was clearly particle size dependent and it increased significantly when particle size was decreased from micrometer to nanometer range. After 10 min, the dissolution of coarse ITZ powder was only  $4.2 \pm 1.2\%$ , whereas the dissolution of ITZ suspensions with particle sizes of 300 nm, 750 nm, and  $5.5 \mu\text{m}$  was  $61.4 \pm 5.3\%$ ,  $43.3 \pm 3.9\%$ , and  $11.2 \pm 2.1\%$ , respectively. Within 90 min, more than 85% of the ITZ nanoparticles of 300 nm size were dissolved, but the dissolution of coarse ITZ powder was still less than 10%. This particle size-dependent dissolution phenomenon can be explained by the larger surface area and potentially higher solubility associated with the nanosuspensions.

#### *In Vivo* Oral Absorption Studies

The plasma concentration–time profiles and the main pharmacokinetic parameters determined for the ITZ nanosuspension are presented in Figure 7 and Table 1. As expected, the oral absorption of coarse ITZ suspension was found to be very low due to its poor dissolution properties. Significant increase in absorption was observed with the nano- and micro-

suspensions. As shown in Table 1, the AUC of ITZ of 300 nm, 750 nm, and  $5.5 \mu\text{m}$  sizes were increased by 50.6, 43.9, and 6.5 times ( $p < 0.05$ ), respectively, when compared with the coarse ITZ powder. Furthermore, enhanced absorption was observed with the nanosuspensions (300 and 750 nm) as compared with the microsuspension ( $5.5 \mu\text{m}$ ). These findings were consistent with the results from the dissolution tests, indicating that the differences in ITZ absorption are primarily attributed to the dissolution behavior of ITZ with different particle sizes. The direct uptake of the drug nanoparticles by mechanisms involving M-cells in Peyer's patches of the gastrointestinal (GI) lymphoid tissue could also be a possible reason for the improved absorption of the nanosized drug particles.<sup>6</sup> This route of drug uptake has also been observed and investigated by other researchers.<sup>24</sup>

It is worth to mention that in spite of a higher  $C_{\text{max}}$  and shorter  $T_{\text{max}}$ , the difference in the extent of absorption (AUC) between the 300- and 750-nm ITZ nanosuspension was statistically insignificant ( $p > 0.05$ ). As shown in Figure 6, the dissolution rate of the 300-nm nanosuspension was significantly higher than that of the 750-nm nanosuspension in the first hour, but the difference became insignificant after the first hour. The higher  $C_{\text{max}}$  and the shorter  $T_{\text{max}}$  are likely attributed to fast initial dissolution of the 300-nm nanosuspension. Because the extent of dissolution for both nanosuspensions was relatively the same after the first hour, there should be sufficient time for complete dissolution and absorption of the drug in the GI tract of the animals regardless of

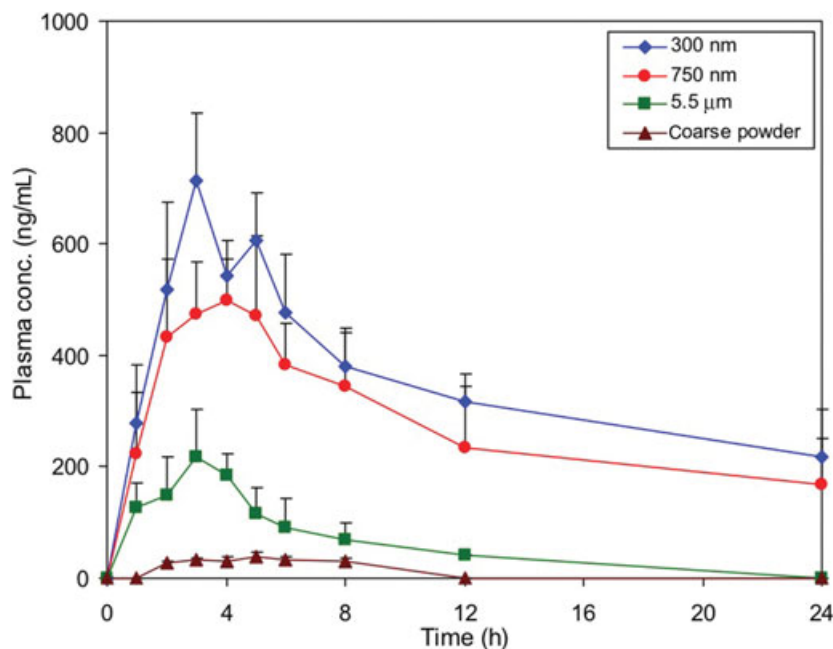


**Figure 7.** Plasma concentration–time profiles of itraconazole after oral administration of suspensions with various particle sizes at a dose of 30 mg/kg body weight in rats ( $n = 3$ ).

**Table 1.** Main Pharmacokinetic Parameters After Oral Administration of Itraconazole Suspensions with Various Particle Sizes in Rats

Formulations	$C_{\max}$ (ng/mL)	$T_{\max}$ (h)	$AUC_{0-24h}$ (ng h/mL)
300 nm	$712 \pm 121$	3	$9967 \pm 2527$
750 nm	$501 \pm 73$	4	$8649 \pm 1580$
5.5 $\mu\text{m}$	$218 \pm 86$	3	$1271 \pm 398$
Powder	$40 \pm 9$	–	$197 \pm 61$

the difference in the initial dissolution rate. This can be the explanation for the similar total drug absorption for these two nanosuspensions.

## CONCLUSIONS

In the present study, ITZ nanosuspensions were prepared by HPH for improving the dissolution and oral absorption of the drug. It was demonstrated that the F127–SLS stabilizer system could be optimized by the use of the central composite design to produce nanosuspensions with maximal particle size reduction. The solid form of ITZ was not altered by the homogenization process. The nanosuspension was physically stable in terms of the particle size at 25°C over 1 week. The dissolution and oral absorption properties of the ITZ suspensions were clearly particle size dependent and both were enhanced significantly when the particle size was reduced to the nanometer range. The results of this study lead to the conclusion that the nanosuspension approach is effective in preparing ITZ formulations with enhanced oral bioavailability.

## ACKNOWLEDGMENTS

This project is financially supported by Abbott Laboratories and the National Basic Research Program of China (973 Program), No. 2009CB930300. We acknowledge Dr. Ping Gao and Dr. John Skoug from Abbott Laboratories for their enlightening discussions and suggestions on this manuscript.

## REFERENCES

- Lipinski C. 2002. Poor aqueous solubility—An industry wide problem in drug discovery. *Am Pharm Rev* 5:82–85.
- Lai F, Sinico C, Ennas G, Marongiu F, Marongiu G, Fadda A. 2009. Diclofenac nanosuspensions: Influence of preparation procedure and crystal form on drug dissolution behaviour. *Int J Pharm* 373:124–132.
- Kesisoglou F, Panmai S, Wu Y. 2007. Nanosizing—Oral formulation development and biopharmaceutical evaluation. *Adv Drug Delivery Rev* 59:631–644.
- Müller RH, Jacobs C, Kayser O. 2001. Nanosuspensions as particulate drug formulations in therapy—Rationale for development and what we can expect for the future. *Adv Drug Delivery Rev* 47:3–19.
- Müller RH, Peters K. 1998. Nanosuspensions for the formulation of poorly soluble drugs: I. Preparation by a size-reduction technique. *Int J Pharm* 160:229–237.
- Rabinow BE. 2004. Nanosuspensions in drug delivery. *Nat Rev Drug Discovery* 3: 785–796.
- Verma S, Lan Y, Gokhale R, Burgess DJ. 2009. Quality by design approach to understand the process of nanosuspension preparation. *Int J Pharm* 377:185–198.
- Van Eerdenbrugh B, Van Den Mooter G, Augustijns P. 2008. Top-down production of drug nanocrystals: Nanosuspension stabilization, miniaturization, and transformation into solid products. *Int J Pharm* 364:64–75.

9. Keck CM, Müller RH. 2006. Drug nanocrystals of poorly soluble drugs produced by high pressure homogenization. *Eur J Pharm Biopharm* 62:3–16.
10. Yoo S, Kang E, Shin B, Jun H, Lee S, Lee KC, Lee K. 2002. Interspecies comparison of the oral absorption of itraconazole in laboratory animals. *Arch Pharm Res* 25:387–391.
11. Jung H, Kim H, Choy YB, Hwang S, Choy J. 2008. Laponite-based nanohybrid for enhanced solubility and controlled release of itraconazole. *Int J Pharm* 349: 283–290.
12. Jung JY, Yoo SD, Lee SH, Kim KH, Yoon DS, Lee KH. 1999. Enhanced solubility and dissolution rate of itraconazole by a solid dispersion technique. *Int J Pharm* 187:209–218.
13. Verreck G, Six K, Mooter GV, Baert L, Peeters J, Brewster ME. 2003. Characterization of solid dispersions of itraconazole and hydroxymethylcellulose prepared by melt extrusion—Part I. *Int J Pharm* 251:165–174.
14. Van Eerdenbrugh B, Froyen L, Van Humbeeck J, Martens JA, Augustijns P, Van Den Mooter G. 2008. Drying of crystalline drug nanosuspensions—The importance of surface hydrophobicity on dissolution behavior upon redispersion. *Eur J Pharm Sci* 35:127–135.
15. Van Eerdenbrugh B, Vermant J, Martens JA, Froyen L, Van Humbeeck J, Augustijns P, Van Den Mooter G. 2009. A screening study of surface stabilization during the production of drug nanocrystals. *J Pharm Sci* 98:2091–2103.
16. Woestenborghs R, Lorreyne W, Heykants J. 1987. Determination of itraconazole in plasma and animal tissues by high-performance liquid chromatography. *J Chromatogr* 413:332–337.
17. Compas D, Touw DJ, de Goede P. 1996. Rapid method for the analysis of itraconazole and hydroxyitraconazole in serum by high-performance liquid chromatography. *J Chromatogr B* 687:453–456.
18. Lee J, Lee SJ, Choi JY, Yoo JY, Ahn CH. 2005. Amphiphilic amino acid copolymers as stabilizers for the preparation of nanocrystal dispersion. *Eur J Pharm Sci* 24:441–449.
19. Van Eerdenbrugh B, Froyen L, Martens JA, Blaton N, Augustijns P, Brewster M, Van Den Mooter G. 2007. Characterization of physicochemical properties and pharmaceutical performance of sucrose co-freeze-dried solid nanoparticulate powders of the anti-HIV agent loviride prepared by media milling. *Int J Pharm* 338:198–206.
20. Kumar MP, Rao YM, Apte S. 2008. Formulation of nanosuspensions of albendazole for oral administration. *Curr Nanosci* 4:53–58.
21. Jackson CL, McKenna GB. 1990. The melting behavior of organic materials confined in porous solids. *J Chem Phys* 93:9002–9011.
22. Van Eerdenbrugh B, Verduyck S, Martens JA, Vermant J, Froyen L, Van Humbeeck G, Van Den Mooter L, Augustijns P. 2008. Microcrystalline cellulose, a useful alternative for sucrose as a matrix former during freeze-drying of drug nanosuspensions—A case study with itraconazole. *Eur J Pharm Biopharm* 70:590–596.
23. Teeranachaideekul V, Junyaprasert VB, Souto EB, Müller RH. 2008. Development of ascorbyl palmitate nanocrystals applying the nanosuspension technology. *Int J Pharm* 354:227–234.
24. Clark MA, Jepson MA, Hirst BH. 2001. Exploiting M cells for drug and vaccine delivery. *Adv Drug Delivery Rev* 50:81–106.